J Neurophysiol 90: 1115–1123, 2003.
First published April 17, 2003; 10.1152/jn.00480.2002.

Features of Neuronal Synchrony in Mouse Visual Cortex

Gabriele Nase,[1] Wolf Singer,[1] Hannah Monyer,[2] and Andreas K. Engel[3]

[1]*Abteilung Neurophysiologie, Max-Planck-Institut für Hirnforschung, 60528 Frankfurt;* [2]*Abt. Klinische Neurobiologie, Universität Heidelberg, 69120 Heidelberg;* [3]*Institut für Neurophysiologie und Pathophysiologie, Universitätsklinikum Hamburg-Eppendorf, 20246 Hamburg, Germany*

Submitted 1 July 2002; accepted in final form 31 March 2003

Nase, Gabriele, Wolf Singer, Hannah Monyer, and Andreas K. Engel. Features of neuronal synchrony in mouse visual cortex. *J Neurophysiol* 90: 1115–1123, 2003. First published April 17, 2003; 10.1152/jn.00480.2002. Synchronization of neuronal discharges has been hypothesized to play a role in defining cell assemblies representing particular constellations of stimulus features. In many systems and species, synchronization is accompanied by an oscillatory response modulation at frequencies in the γ-band. The cellular mechanisms underlying these phenomena of synchronization and oscillatory patterning have been studied mainly in vitro due to the difficulty in designing a direct in vivo assay. With the prospect of using conditional genetic manipulations of cortical network components, our objective was to test whether the mouse would meet the criteria to provide a model system for the study of γ-band synchrony. Multi-unit and local field potential recordings were made from the primary visual cortex of anesthetized C57BL/6J mice. Neuronal responses evoked by moving gratings, bars, and random dot patterns were analyzed with respect to neuronal synchrony and temporal patterning. Oscillations at γ-frequencies were readily evoked with all types of stimuli used. Oscillation and synchronization strength were largest for gratings and decreased when the noise level was increased in random-dot patterns. The center peak width of cross-correlograms was smallest for bars and increased with noise, yielding a significant difference between coherent random dot patterns versus patterns with 70% noise. Field potential analysis typically revealed increases of power in the γ-band during response periods. Our findings are compatible with a role for neuronal synchrony in mediating perceptual binding and suggest the usefulness of the mouse model for testing hypotheses concerning both the mechanisms and the functional role of temporal patterning.

INTRODUCTION

Visual cortex neurons are able to synchronize their discharge with millisecond precision. Often, synchronization is associated with oscillatory modulation of spike firing in the γ-frequency range (>30 Hz) (Gray et al. 1989). The coordination of spike timing is generated intracortically and dependent on global stimulus properties (for review see Engel and Singer 2001; Engel et al. 2001; Singer 1999; Singer and Gray 1995). Therefore it is not a mere reflection of network connectivity but, rather, a result of context-dependent dynamic interactions involving a combination of bottom-up and top-down influences (reviewed in Engel et al. 2001). It has been proposed to provide a general mechanism by which activity patterns in spatially separate regions of the brain are temporally coordinated (Gray et al. 1989; Singer and Gray 1995). Dynamic cell assemblies formed by synchronously firing neurons would signal to subsequent processing stages the relatedness of their responses, thus establishing relations among features of perceptual objects and favoring further joint processing due to the increased saliency of the correlated responses (for review see Singer 1999; Singer and Gray 1995).

Such precise stimulus-induced synchronization is not restricted to the mammalian visual system. Rather, it represents a common phenomenon across species and has, for instance, also been found in the visual system of reptiles (Prechtl 1994) and birds (Neuenschwander and Varela 1993). Moreover, these findings can be generalized across neural systems. Thus synchronization is well known to occur in the olfactory system of various vertebrate and invertebrate species, where these phenomena have been related to the processing of odor information (Freeman 1988; Laurent 1996). Moreover, in both the auditory (deCharms and Merzenich 1996; Eggermont 1992) and the somatosensory cortex (Nicolelis et al. 1995; Steriade et al. 1996) precise neuronal synchronization has been observed. Furthermore, neuronal interactions with a precision in the millisecond range have been described in the hippocampus (Bragin et al. 1995; Buzsáki and Chrobak 1995), in the frontal cortex (Abeles et al. 1993; Vaadia et al. 1995), and in the motor system where neural synchronization has been discovered during both preparation and execution of movements (Murthy and Fetz 1992; Riehle et al. 1997; Sanes and Donoghue 1993). Recent electroencephalographic (EEG) and magnetoencephalographic (MEG) studies indicate that stimulus-induced synchronization at γ-frequencies is also present in the human brain (for review see Tallon-Baudry and Bertrand 1999) and occurs during auditory (Galambos et al. 1981; Pantev et al. 1991), visual (Herrmann et al. 1999; Müller et al. 1997; Rodriguez et al. 1999; Tallon-Baudry et al. 1997), and language processing (Pulvermüller et al. 1995) as well as during execution of motor tasks (Kristeva-Feige et al. 1993).

Despite their widespread occurrence and hypothesized importance, the cellular mechanisms underlying the phenomena of stimulus-induced synchronization and oscillatory patterning of neural responses remain poorly understood. Mice are especially well suited as a model organism for the exploration of cellular mechanisms due to the possibility of targeted genetic manipulation. The majority of data related to neuronal synchrony and γ-oscillations has been obtained from the visual

Address for reprint requests: G. Nase, Abt. Neurophysiologie, Max-Planck-Institut für Hirnforschung, Deutschordenstr. 46, 60528 Frankfurt, Germany (E-mail: nase@mpih-frankfurt.mpg.de).

The costs of publication of this article were defrayed in part by the payment of page charges. The article must therefore be hereby marked "*advertisement*" in accordance with 18 U.S.C. Section 1734 solely to indicate this fact.

cortices of cat and monkey. Our objective was to test whether the mouse could provide a model system in this context. Ideally, neurons in the mouse visual cortex would possess functional features similar to those found in cat and monkey (i.e., be able to synchronize their activity in a stimulus-related fashion and to engage in stimulus-induced γ-oscillations). Here we report the first in vivo study of synchronization and γ-oscillations in the mouse and provide a baseline suitable for comparison with data from mutant mice. Portions of this work have previously appeared in abstract form (Nase et al. 1999).

METHODS

Animals

In total, 65 adult C57Bl/6J mice of either sex were used in the study. Animals were obtained from Charles River Deutschland GmbH, Sulzfeld, Germany. All experimental procedures were in accordance with the German Law for the Protection of Experimental Animals and conformed with the Guiding Principles for Research Involving Animals and Human Beings embodied in the Declaration of Helsinki.

Preparation, anesthesia, and surgical procedures

Experimental procedures for recording from mouse visual cortex were adapted from Drager (1975) and Gordon and Stryker (1996). After induction of anesthesia with ketamine (Ketanest, Parke-Davis, Courbevoie, France; 10 mg/kg, ip) and xylazine (Rompun, Bayer, Wuppertal, Germany; 2 mg/kg, ip), a tracheotomy was made for artificial ventilation, and the animal was placed in a stereotaxic apparatus. Throughout surgery and during the recordings, general anesthesia was maintained by ventilating the animal with a mixture of 50% N_2O and 50% O_2 supplemented by 0.4–1.0% halothane or 0.6–1.0% isoflurane. Body temperature was kept in the range of 36.8–37.2°C. A recording chamber was mounted on the skull and a craniotomy was made exposing area 17. The dura was left intact and covered with agar and silicon oil. Following surgery, paralysis was induced and maintained by subcutaneous infusion of pancuronium bromide (Pancuronium, Organon Teknika-Cappel, Malvern, PA; 1 $mg \cdot kg^{-1} \cdot h^{-1}$, sc). Ventilation pressure and electrocardiogram were monitored continuously. The cornea was protected from drying with silicone oil throughout the course of the experiment. Slight mydriasis was present throughout the experiment, presumably caused by the administered xylazine. In physiologically stable animals, strong neuronal responses were readily obtained through a recording period of 8–10 h. Only when ECG abnormalities or corneal cataracts developed, responsiveness declined. Such experiments were then terminated.

Visual stimulation and experimental design

Stimulation was monocular. Visual stimuli were computer generated and back-projected onto a tangent screen 28 cm in front of the animal at an angle of 60° with respect to the animals' midline (frame rate, 60 Hz; background luminance, 3.3 $cd \cdot m^{-2}$; frame size, 80 by 80°, duration 2.2 s). Stimuli comprised bars (width, 4°; length 60°, contrast 0.96; velocity, 20°/s), sinusoidal drifting gratings (size, 70 by 70°; spatial frequency, 0.1 cycles/°; temporal frequency, 5 cycles/s; contrast, 0.66), and random dot patterns (area coverage, 10%; dot size, 0.6 by 0.6°; velocity, 20°/s) with or without visual noise. Directional tuning was tested for with different directions of motion of the respective stimulus (in steps of 45°). The direction of movement of the bars and gratings was always kept perpendicular to their orientation. Each stimulus was presented ≥10 times. Stimulus presentations were interleaved in a block-wise randomized fashion. Individual sessions lasted approximately 1–1.5 h.

Multiple-electrode recordings

Multi-unit activity (MUA) was recorded with tungsten electrodes (impedance 0.4–0.8 MΩ) placed within the primary visual cortex. Four electrodes were used simultaneously. The electrodes were arranged in a square with an edge length of 200–250 μm. The separation, therefore, ranged approximately between 200 and 350 μm, with electrodes connected by an "edge" of the square closer together and the electrodes connected by a "diagonal" slightly further apart. The electrode signal was amplified and band-pass filtered between 1 and 3 kHz, fed through a Schmitt trigger whose threshold was set higher than twice the noise level, and the trigger pulses were sampled at 2 kHz. Simultaneously, local field potentials (LFP) were recorded from the same electrodes by band-pass filtering of the raw signals between 1 and 100 Hz. The signals were digitized at 2 kHz using a 1401 CED interface controlled by Spike2 software (Cambridge Electronic Design, Cambridge, UK) and stored on computer disk for off-line analysis.

Data analysis

Off-line analysis was performed using LabVIEW (National Instruments, Austin, TX) and IDL (Research Systems, Boulder, CO). Oscillatory response modulation and synchronization were analyzed by computing and averaging auto- and cross-correlograms for all trials per condition and recording site with a bin size of 1 ms. To avoid inclusion of nonstationary, phasic response components, the first 200 ms after visual stimulus onset were discarded before analysis. In addition, shift-predictor correlograms were calculated. Since these were consistently flat, quantification was carried out using raw correlograms without subtraction of shift-predictors. For quantification of the correlogram modulation, a damped cosine (Gabor) function was fitted to the correlograms (König 1994). The fitted function had to account for ≥15% of the data variance and the *z*-scores of significant peaks had to be >2. The strength of oscillatory modulation was assessed from the ratio of the amplitude of the first satellite peak over the offset of the function fitted to the auto-correlograms, yielding the modulation amplitude of the first satellite peak (MAS). Similarly, synchronization strength was evaluated using the modulation amplitude (MA) of the central peak in the correlograms (i.e., the ratio between the peak amplitude and offset of the fitted function). In addition, frequency of oscillation, phase shift of the modulation, and width of center and first satellite peak, respectively, were determined using parameters of the fitted function.

To visualize the development of oscillatory patterning and response synchronization over time, a sliding window analysis was performed by moving a short analysis window (200 ms) in successive steps (50 ms) over the responses. The correlograms obtained for each of those windows are plotted in a two-dimensional graph, where the *y*-axis denotes the time shift of the correlation and the *x*-axis denotes the time course of the responses. The amplitudes of the correlogram peaks are displayed with a color code (see Fig. 4).

The LFPs were analyzed with respect to their spectral composition and their correlation with the MUA. The relative power of the LFP during baseline activity and during response epochs was assessed by calculating normalized power spectra for the respective time intervals. Bins from 25–48 Hz were summed up to obtain a measure for the relative power in the γ-frequency band. As a measure of synchronization between MUA and LFP, the spike-field coherence (SFC) (Fries et al. 1997) was computed. First, spike-triggered averages (STAs) were computed by averaging the LFPs within an analysis window of ±128 ms centered on each trigger spike. Second, spike-triggered power spectra (STPs) were obtained by averaging of the power spectra of the LFP segments used for the computation of the STAs. Finally, the SFC was obtained as the ratio of the power spectrum of the STA over the STP. The SFC is unitless and ranges between zero for lack of phase synchronization and one for total phase synchroni-

zation. As a measure for SFC in the γ-frequency range, the values from 25–48 Hz were summed up.

RESULTS

Temporal patterning of visual responses

Data from a total of 206 recording sites were analyzed for the presence of oscillatory responses. At the majority of sites, oscillations were readily evoked by visual stimuli and were easily detectable in both MUA and LFPs of individual trials by visual inspection. As illustrated in Fig. 1, the spikes of the MUA are clustered in bursts that recur at γ-frequencies. A typical observation is that the spikes are phase-locked to the negative peaks of the LFP oscillations. Our data sample comprised a total of 159 pairs of MUA recordings that were used for cross-correlation analysis. As shown in Fig. 2, γ-oscillations at individual recording sites could be highly synchronous, yielding a strongly modulated cross-correlogram. Computation of shift-predictors revealed that neither the oscillations nor the synchronized spikes were phase-locked to the visual stimuli, as indicated by the absence of modulation in the shift-predictor correlograms (Fig. 2*b*).

Dynamic variability of correlation patterns

Both the strength and the frequency of oscillatory modulation and the degree of synchronization between different recording sites displayed noticeable inter-trial variability. Typically, 10 trials with identical stimuli were recorded in a time window of 60–90 min (randomly interleaved with trials where other stimuli were shown, cf. METHODS). In a number of cases, the modulation of cross-correlograms was investigated on a trial-by-trial basis. An example for such a single-trial analysis is illustrated in Fig. 3. In this case, most of the trials displayed significant synchronization, accompanied by oscillatory modulation with slightly varying frequency. Four of the trials showed either a flat correlogram or only a center peak, indicating nonoscillatory synchronization. The neuronal firing

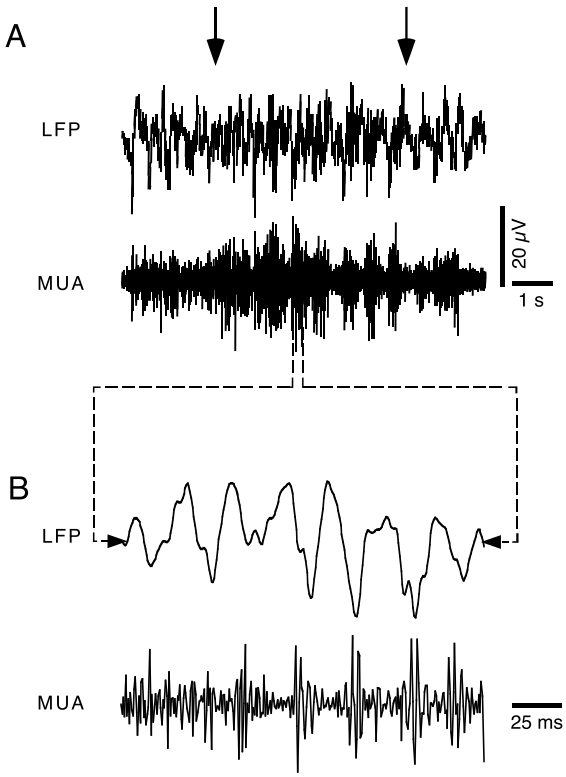

FIG. 1. Neuronal γ-oscillations in mouse visual cortex. Multi-unit and local field potential responses to a drifting grating were recorded from area 17 in an adult C57BL/6J mouse. The figure shows traces from a single trial at compressed time scale (*a*) and at an expanded time scale (*b*). Arrows in *a* indicate the onset and offset of visual stimulation, respectively. Note the presence of rhythmic oscillations (approximately 40 Hz) in the local field potential and the multi-unit activity.

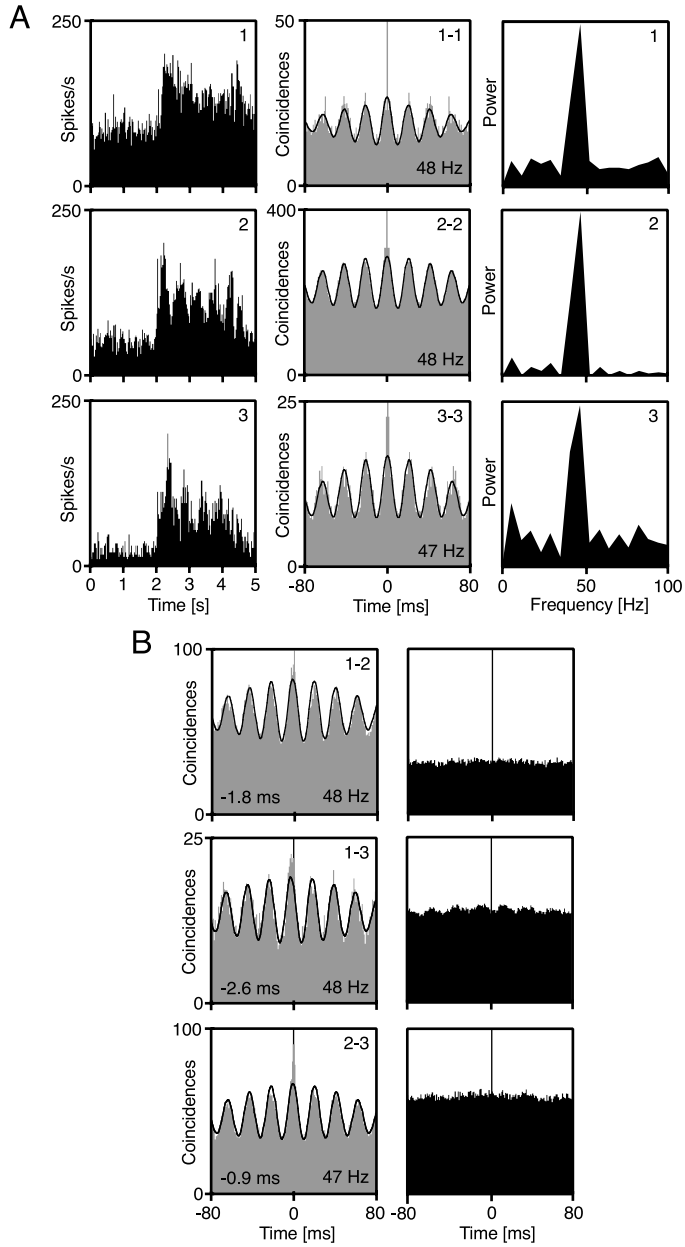

FIG. 2. Multi-unit activity (MUA) correlation analysis. In this example, simultaneous recordings of three multi-units responding to a drifting grating were obtained. *a*: peri-stimulus-time histograms (*left*), auto-correlograms (*middle*), and power spectra of the auto-correlograms (*right*) for the 3 responses. *b*: cross-correlograms for the 3 possible pairwise combinations. The right column shows the shift-predictors for the 3 respective cross-correlograms. Numbers indicate the dominant frequency of the oscillatory modulation (*a*, *b*) and the phase-shift of the center peak (*b*) for the correlograms. These values were obtained from the Gabor function (continuous lines) fitted to the data.

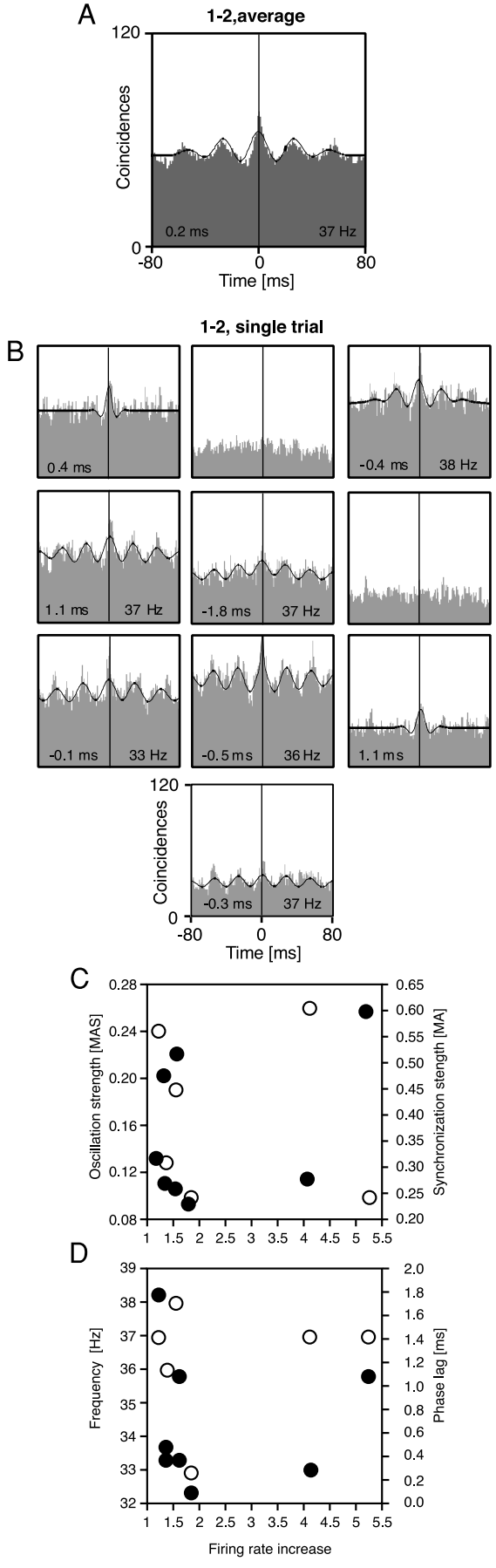

rates also showed some variation across trials but there was no obvious relationship between activation levels and the degree of temporal patterning in the responses (Fig. 3, *c* and *d*), as revealed by computing the correlation between the firing rate and the other parameters. These correlation coefficients were 0.04 for oscillation frequency, 0.01 for oscillation strength, 0.16 for synchronization strength, and 0.0002 for the absolute value of the phase lag, respectively.

Sliding-window analysis

Using sliding-windows for computation of average cross-correlograms (cf. METHODS), we investigated the oscillatory patterning in multi-unit activity and the temporal correlation between pairs of MUAs along the stimulation epochs (Fig. 4). This analysis typically showed that oscillatory patterning and response synchronization had a rapid onset and lasted throughout the response epochs. In many cases, oscillation frequency decreased during sustained responses. The highest oscillation frequency typically occurred immediately at response onset, even if the maximum firing rates had not yet been achieved. Averaged across our entire data sample, however, this decrease in frequency was not significant, and oscillation frequencies were always within the γ-band.

Analysis of local field potentials

LFPs consistently revealed the same temporal patterning as the unit activity. For all stimulus conditions, power spectra exhibited an oscillatory modulation at approximately 40 Hz and significant increases in power in the γ-band during response periods as compared with baseline activity ($P < 0.0001$, Wilcoxon signed-rank test) (Fig. 5*a*). The magnitude of the stimulus-induced increase in power at γ-frequencies was maximal in response to bars and declined significantly with the coherence of the random dot stimuli ($P < 0.005$ for random dot patterns without vs. with 30% visual noise, and $P < 0.0001$ for random dot patterns without vs. with 70% visual noise, Wilcoxon signed-rank test) (Fig. 5*b*). We computed STAs of the LFPs and their corresponding power spectra. For all tested stimulus conditions, an oscillatory modulation in the γ-frequency range was observed. However, no significant differences occurred in the SFCs for the different stimulus conditions. SFC at γ-frequencies ranged between 0.01 and 0.20 and was 0.09 ± 0.01 for bars, 0.08 ± 0.01 for gratings, 0.08 ± 0.01 random dot patterns, and 0.08 ± 0.01 and 0.08 ± 0.01 for random dot patterns with 30 and 70% noise, respectively (mean ± SE).

FIG. 3. Intertrial variability. Ten successive trials with identical stimulus were analyzed. *a*: the average correlogram shows a prominent center peak and significant oscillatory modulation with a frequency of 37 Hz. (*b*) Many cross-correlograms of individual trials showed a center peak and significant oscillatory modulation ranging from 33 to 38 Hz. Continuous lines represent the Gabor function fitted to the data. Numbers indicate the dominant frequency of the oscillatory modulation and the phase-shift of the center peak. *c*: scatter plots showing the relation between the neuronal firing rates and oscillation strength (open circles) or strength of synchrony (filled circles), respectively. *d*: relation between firing rates and oscillation frequency (open circles) and phase lag (filled circles). The respective correlation coefficients are 0.11 for oscillation frequency, 0.08 for oscillation strength, 0.11 for synchronization strength, and 0.03 for the absolute value of the phase lag.

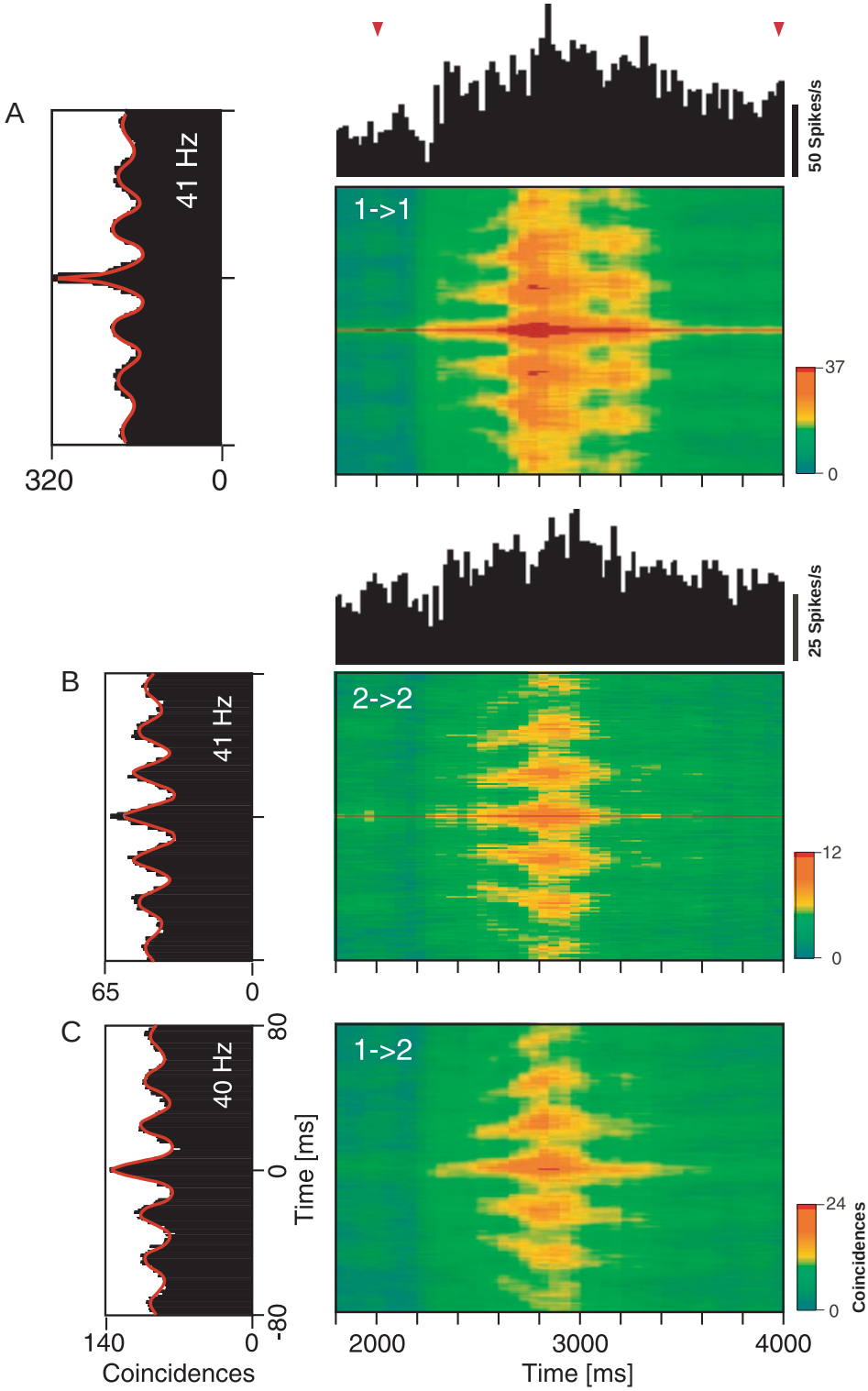

FIG. 4. Oscillatory patterning and synchronization during sustained responses. The plots show the development of oscillatory patterning in the multi-unit activity at 2 separate sites (*a*) and (*b*) and the response synchronization (*c*) over time, averaged for 10 trials with identical stimuli. Correlograms were computed for a window sliding along the time axis, and positive correlogram peaks are displayed with red-orange colors. The *y*-axis denotes the time shift of the correlation and the *x*-axis denotes the time course of the responses. To the left of each sliding-window plot, the averaged correlograms are shown, the number indicating the peak oscillation frequency. Peristimulus-time histograms (PSTHs) are also shown for the 2 sites. The cells were stimulated with a moving bar, displayed during the time period denoted by the red arrowheads. Oscillatory patterning and response synchronization had a rapid onset and lasted throughout the response epochs.

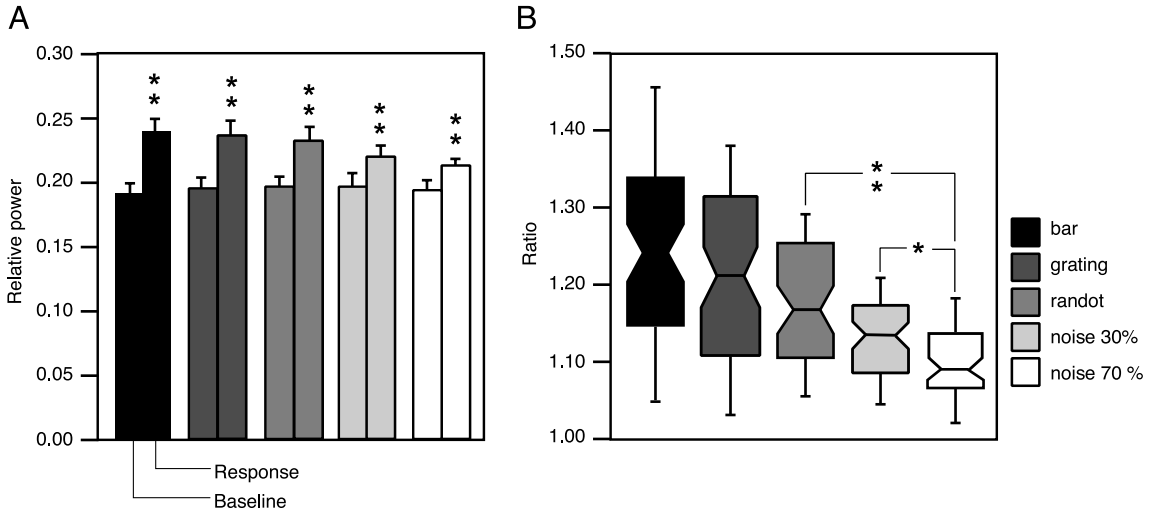

FIG. 5. Stimulus-dependent increase in local field potentials (LFP) power at γ-frequencies. *a*: comparisons of relative power in the γ-frequency band during baseline and response to bars, gratings, and random dot patterns without and with 30 and 70% visual noise ($n = 68$, error bars denote SE) reveal a significant increase ($P < 0.0001$, Wilcoxon signed-rank test) for all stimulus conditions (**). *b*: the ratio of relative power at γ-frequencies during response epochs and baseline is shown for all stimulus conditions. The horizontal tick within each box denotes the median; its lower and upper orders denote the 25th and 75th percentile, and ticks below and above the boxes denote the 10th and 90th percentile of the distribution. Notches in the boxes indicate the 95% confidence interval. The magnitude of the stimulus-induced increase was maximal in response to bars and declined significantly as the visual noise in random dot patterns increased from 0 to 30% (*, $P < 0.005$) and 70% (**, $P < 0.001$, Wilcoxon signed-rank test).

Quantitative analysis of temporal patterning in unit activity

Oscillations at γ-frequencies were readily induced with all types of stimuli used, provided that the stimuli had yielded sufficient activation of the neurons to permit correlation analysis. Oscillatory patterning was comparable for randomly interleaved responses to bars, gratings, and random dot patterns. Although synchrony and oscillations were readily observed if random dot patterns contained visual noise, the temporal precision of spike synchronization was reduced with this stimulus type.

The collective incidence of oscillations and synchrony for all stimuli used is illustrated in Fig. 6. A significant oscillatory modulation was observed at 126 recording sites (61%, $n = 206$) (Fig. 6*a*). In none of the cases was the oscillatory modulation phase-locked to visual stimulus onset. Cross-correlation analysis showed that 129 pairs of recording sites (81%, $n = 159$) exhibited significant response synchronization (Fig. 6*b*). Shift-predictor controls did not show significant center peaks. In all cases, synchrony was stimulus induced and not present during spontaneous activity. The incidence of oscillations in cross-correlograms was comparable to that found for auto-correlograms. An oscillatory modulation in the γ-frequency range was observed in 67% ($n = 106$) of the synchronized responses (Fig. 6*c*). In most cases (65%, $n = 104$) synchronization occurred together with γ-oscillations; in 25 cases (16%) synchronization was not accompanied by γ-oscillations and in two cases (1%) γ-oscillations occurred without synchronization between sites (Fig. 6*d*).

Figure 7 summarizes the statistical analysis of the firing rates, oscillation frequencies, center peak width, oscillation strength, and strength of synchrony for the different stimulus types. The indices for oscillations and synchrony were extracted from the Gabor functions fitted to the auto- and cross-correlograms. Firing rates did not differ significantly for the various stimulus classes (Fig. 7*a*). Oscillation frequencies were most common in the range of 35–40 Hz and similar across all stimuli (range 25–50 Hz) (Fig. 7*b*). These oscillations are of intrinsic origin since there was no evidence for phase-locking

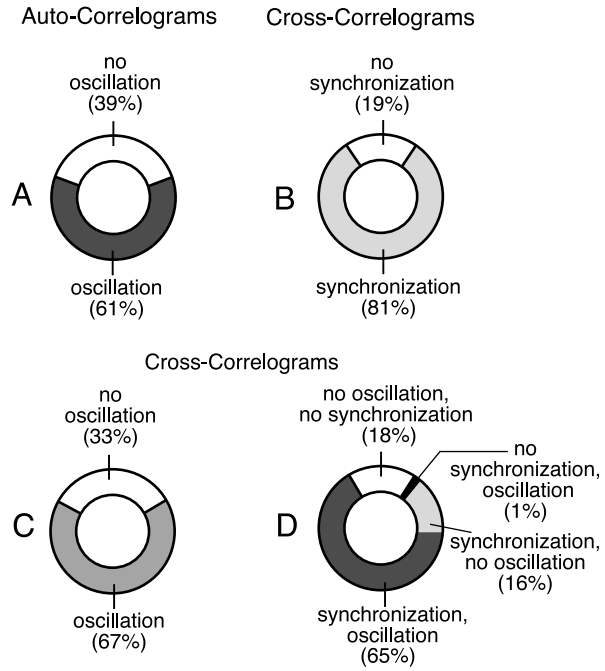

FIG. 6. Incidence of oscillation and synchronization. *a*: significant oscillatory modulation was observed at 126 of 206 recording sites in at least 1 averaged auto-correlogram. *b*: of a total of 159 pairs of recording sites, 129 exhibited significant response synchronization in at least 1 averaged cross-correlogram. *c*: in 106 of these cases, cross-correlograms showed an oscillatory modulation in the γ-frequency range. *d*: in most cases ($n = 104$) synchronization, as indicated by a significant center peak, occurred together with γ-oscillations.

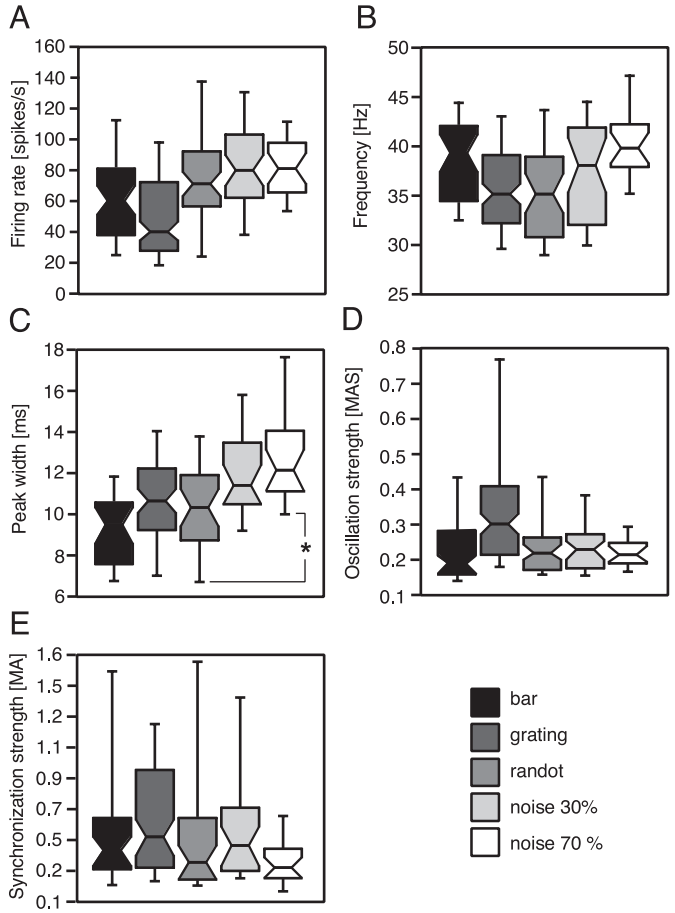

FIG. 7. Parameters of synchronized activity under different stimulus conditions. For 90 pairs of recording sites the geometric mean of the firing rate of target and reference (*a*), the oscillation frequency (*b*), the oscillation strength (*c*), the synchronization strength (*d*), and the center peak width (*e*) had been determined. The horizontal tick within each box denotes the median; its top and bottom borders denote the 25th and 75th percentile, respectively. Ticks below and above the boxes indicate the 10th and 90th percentile of the distribution. Notches in the boxes indicate the 95% confidence interval. Note that the center peak width of the cross-correlograms (*c*) increased with visual noise, yielding a significant difference (*) between coherent random dot patterns vs. patterns with 70% visual noise ($P < 0.005$, Wilcoxon signed-rank test).

to stimulus transients and since oscillation frequencies were well below the frame rate (60Hz) of the stimulus projector. Synchronization of responses to coherent stimuli consistently had millisecond precision, as shown by the analysis of the center peak width in the cross-correlograms. For single bars and gratings, peak width was typically in the range of 7 to 14 ms (Fig. 7*c*). However, the width of the center peaks increased with visual noise, yielding a significant difference between random dot patterns without noise and patterns with 70% visual noise ($P < 0.005$, Wilcoxon signed-rank test). Both oscillation and synchronization strength (Fig. 7, *d* and *e*) were maximal for gratings. Across animals (mice with ≥10 different pairs of analyzed recording sites), no significant differences were observed in oscillation strength, synchronization strength, and center peak width.

DISCUSSION

We present the first report that neurons in the visual cortex of mice engage in γ-oscillations and synchronize their firing in response to visual stimulation. Furthermore, we demonstrate the feasibility of correlation analysis of visually evoked unit activity recorded in vivo in the mouse and provide a full characterization of the features of stimulus-induced γ-oscillations and neuronal synchronization in this species.

Oscillations and synchrony are robust phenomena in the mouse

Neurons in the visual cortex of mice display stimulus-induced γ-oscillations and neuronal synchronization that can be readily evoked using standard stimuli. In most cases light responsive neurons exhibited stimulus-evoked oscillatory firing in the γ-frequency range, and the majority of analyzed co-activated multi-unit pairs showed response synchronization with millisecond precision. Similar parameters of stimulus-induced oscillatory patterning and spike time coordination were detected in all analyzed mice and were present throughout the duration of the respective experiments. This demonstrates that oscillatory patterning and synchronization of responses represent robust phenomena in the primary visual cortex of mice. The relative ease of eliciting γ-frequency oscillations and response synchronization might be related to the fact that neurons in the primary visual cortex of the mouse have large receptive fields and are less selective (Drager 1975; Metin et al. 1988; Wagor et al. 1980) than neurons in cat or monkey primary visual cortex (Hubel and Wiesel 1962, 1968) regarding stimulus properties such as orientation and direction of movement. Therefore it becomes more likely to encounter neurons with similar preferences, yielding a relatively high incidence of spike time coordination locally and between pairs of electrodes. Nevertheless, correlation patterns in primary visual cortex of the mouse are dependent on stimulus conditions.

Rapid and reliable assessment of correlation patterns

The little time and effort needed to complete the in vivo preparation in the mouse as compared with similar experiments in cats allows for the assessment of the respective parameters of oscillatory patterning and synchrony at multiple sites in large numbers of animals, which is a basic requirement when probing the effect of a gene mutation on these parameters. In addition, it is important to apply standard methods for the independent evaluation of synchronization and oscillatory patterning to obtain robust quantitative values for statistical assessment. To this end, we employed a method devised by König which involves fitting Gabor functions to the correlograms, the details of which have been discussed elsewhere (König 1994). Furthermore, the collected data in the study compare well across individual experimental animals, which constitutes an additional requirement for rapid and reliable screening of changes of temporal patterning in genetically modified animals. Taken together, it seems feasible to compare correlation patterns of visually evoked activity among mutant and wild-type mice.

Similarities to cat and monkey

Numerous physiological studies have addressed the characterization of patterns of coordination in spike timing among cortical neurons (reviewed in Engel et al. 2001; Singer 1999;

Singer and Gray 1995). The present results of temporal firing behavior from mouse primary visual cortex neurons are in good agreement with data obtained in related studies in awake (Fries et al. 1997; Gray and Viana Di Prisco 1997) and anesthetized cats (Eckhorn et al. 1988; Gray and Singer 1989; Gray et al. 1989; Steriade et al. 1996) and monkeys (Frien et al. 1994; Kreiter and Singer 1996; Maldonado et al. 2000). Correlation patterns in the mouse visual cortex are as precise as in cats, and as in cats (Engel et al. 2000), the precision of temporal coincidences reflects stimulus coherence. With decreasing coherence of motion in random dot patterns, the width of the center peak increased. The other parameters obtained from the fitted Gabor functions such as the synchronization strength, oscillation frequency, oscillation strength, and phase lag agree well with the corresponding values in cat and monkey visual cortex (Eckhorn et al. 1988; Engel et al. 1990; Friedman-Hill et al. 2000; Frien et al. 1994; Gray and Singer 1989; Gray et al. 1989; Kreiter and Singer 1996; Maldonado et al. 2000). The same was true for the time course of the correlation patterns. Oscillations and synchronization had a rapid onset, were present throughout the response period (Gray et al. 1992), and showed a progressive decay in frequency (Castelo-Branco et al. 1998). The correlation patterns observed in mice also exhibit some degree of variation from one trial to the next, which is a typical feature also in anesthetized and awake preparations of higher mammals (Engel et al. 1990).

However, we also found two noteworthy differences of the correlation patterns in the mouse as compared with those in the cat. One difference concerns the frequency of the evoked oscillations. In mouse visual cortex we did not measure frequencies higher than 55 Hz and in most cases the oscillation frequency was below 50 Hz. These values are lower than those reported for oscillation frequencies in the anesthetized (Gray and Singer 1989) and awake cat (Fries et al. 1997; Gray and Viana Di Prisco 1997), where values $\leq$70 Hz are frequently observed. Moreover, neurons in mouse primary visual cortex did not display the high-frequency oscillations of retinal origin (Castelo-Branco et al. 1998; Neuenschwander and Singer 1996), suggesting either a lack of retinal oscillations or an inability of the intra-cortical circuitry to follow such high frequencies. A second difference concerns the incidence of γ-frequency oscillations and of response synchronization. In mice, recording sites exhibiting oscillatory firing and/or synchronized firing were encountered more frequently than in the cat (Engel et al. 1990; Gray and Singer 1989; Gray et al. 1989). The higher incidence of correlated firing probably relates to the lower degree of functional segregation within mouse visual cortex, as evident from rather uniform response characteristics and the apparent lack of columnar clustering, consistent with findings in rat primary visual cortex (Girman et al. 1999).

In conclusion, the results presented here confirm the notion that stimulus-induced γ-oscillations and neuronal synchronization are a general phenomenon. In mice, these correlation patterns exhibit the hallmarks reported for other species. Therefore the mouse can serve as a model for testing hypotheses concerning both the mechanisms and the functional role of stimulus-induced γ-oscillations and neuronal synchronization.

We thank M. P. Stryker, J. L. Hannover, P. Fries, and M. Brecht for technical advice; S. Neuenschwander and M. Stephan for help with data analysis; J. Klon-Lipok for technical assistance; and R. Ruhl for help in preparing the figures.

DISCLOSURES

This work was supported by the Max-Planck-Society and the Deutsche Forschungsgemeinschaft (Mo 432/4-1, En 203/4-2).

REFERENCES

Abeles M, Vaadia E, Bergman H, Prut Y, Haalman I, and Slovin H. Dynamics of neuronal interactions in the frontal cortex of behaving monkeys. *Concepts Neurosci* 4: 131–158, 1993.

Bragin A, Jandó G, Nádasdy Z, Hetke J, Wise K, and Buzsáki G. Gamma (40–100 Hz) oscillation in the hippocampus of the behaving rat. *J Neurosci* 15: 47–60, 1995.

Buzsáki G and Chrobak JJ. Temporal structure in spatially organized neuronal ensembles: a role for interneuronal networks. *Curr Opin Neurobiol* 5: 504–510, 1995.

Castelo-Branco M, Neuenschwander S, and Singer W. Synchronization of visual responses between the cortex, lateral geniculate nucleus, and retina in the anesthetized cat. *J Neurosci* 18: 6395–6410, 1998.

deCharms RC and Merzenich MM. Primary cortical representation of sounds by the coordination of action-potential timing. *Nature* 381: 610–613, 1996.

Drager UC. Receptive fields of single cells and topography in mouse visual cortex. *J Comp Neurol* 160: 269–290, 1975.

Eckhorn R, Bauer R, Jordan W, Brosch M, Kruse W, Munk M, and Reitboeck HJ. Coherent oscillations: a mechanism of feature linking in the visual cortex? Multiple electrode and correlation analyses in the cat. *Biol Cybern* 60: 121–130, 1988.

Eggermont JJ. Neural interaction in cat primary auditory cortex. Dependence on recording depth, electrode separation, and age. *J Neurophysiol* 68: 1216–1228, 1992.

Engel AK, Fries P, and Singer W. Dynamic predictions: oscillations and synchrony in top-down processing. *Nat Rev Neurosci* 2: 704–716, 2001.

Engel AK, Kluge T, Fickel U, and Goebel R. Responses and temporal patterning with motion-contrast stimuli in cat extrastriate visual cortex. *Soc Neurosci Abstr* 26: 251, 2000.

Engel AK, König P, Gray CM, and Singer W. Stimulus-dependent neuronal oscillations in cat visual cortex: inter-columnar interaction as determined by cross-correlation analysis. *Eur J Neurosci* 2: 588–606, 1990.

Engel AK and Singer W. Temporal binding and the neural correlates of sensory awareness. *Trends Cognit Sci* 5: 16–25, 2001.

Freeman WJ. Nonlinear neural dynamics in olfaction as a model for cognition. In: *Dynamics of Sensory and Cognitive Processing by the Brain*, edited by Basar E. Berlin: Springer, 1988, p. 19–29.

Friedman-Hill S, Maldonado PE, and Gray CM. Dynamics of striate cortical activity in the alert macaque. I. Incidence and stimulus-dependence of gamma-band neuronal oscillations. *Cereb Cortex* 10: 1105–1116, 2000.

Frien A, Eckhorn R, Bauer R, Woelbern T, and Kehr H. Stimulus-specific fast oscillations at zero phase between visual areas V1 and V2 of awake monkey. *Neuroreport* 5: 2273–2277, 1994.

Fries P, Roelfsema PR, Engel AK, Konig P, and Singer W. Synchronization of oscillatory responses in visual cortex correlates with perception in interocular rivalry. *Proc Natl Acad Sci USA* 94: 12699–12704, 1997.

Galambos R, Makeig S, and Talmachoff PJ. A 40-Hz auditory potential recorded from the human scalp. *Proc Natl Acad Sci U S A* 78: 2643–2647, 1981.

Girman SV, Sauve Y, and Lund RD. Receptive field properties of single neurons in rat primary visual cortex. *J Neurophysiol* 82: 301–311, 1999.

Gordon JA and Stryker MP. Experience-dependent plasticity of binocular responses in the primary visual cortex of the mouse. *J Neurosci* 16: 3274–3286, 1996.

Gray CM, Engel AK, König P, and Singer W. Synchronization of oscillatory neuronal responses in cat striate cortex: temporal properties. *Vis Neurosci* 8: 337–347, 1992.

Gray CM, Konig P, Engel AK, and Singer W. Oscillatory responses in cat visual cortex exhibit inter-columnar synchronization which reflects global stimulus properties. *Nature* 338: 334–337, 1989.

Gray CM and Singer W. Stimulus-specific neuronal oscillations in orientation columns of cat visual cortex. *Proc Natl Acad Sci USA* 86: 1698–1702, 1989.

Gray CM and Viana Di Prisco G. Stimulus-dependent neuronal oscillations and local synchronization in striate cortex of the alert cat. *J Neurosci* 17: 3239–3253, 1997.

Herrmann CS, Mecklinger A, and Pfeifer E. Gamma responses and ERPs in a visual classification task. *Clin Neurophysiol* 110: 636–642, 1999.

Hubel DH and Wiesel TN. Receptive fields, binocular interaction and functional architecture in the cat's visual cortex. *J Physiol* 160: 106–154, 1962.

Hubel DH and Wiesel TN. Receptive fields and functional architecture of monkey striate cortex. *J Physiol* 195: 215–243, 1968.

König P. A method for the quantification of synchrony and oscillatory properties of neuronal activity. *J Neurosci Methods* 54: 31–37, 1994.

Kreiter AK and Singer W. Stimulus-dependent synchronization of neuronal responses in the visual cortex of the awake macaque monkey. *J Neurosci* 16: 2381–2396, 1996.

Kristeva-Feige R, Feige B, Makeig S, Ross B, and Elbert T. Oscillatory brain activity during a motor task. *Neuroreport* 4: 1291–1294, 1993.

Laurent G. Dynamical representation of odors by oscillating and evolving neural assemblies. *Trends Neurosci* 19: 489–496, 1996.

Maldonado PE, Friedman-Hill S, and Gray CM. Dynamics of striate cortical activity in the alert macaque. II. Fast time scale synchronization. *Cereb Cortex* 10: 1117–1131, 2000.

Metin C, Godement P, and Imbert M. The primary visual cortex in the mouse: receptive field properties and functional organization. *Exp Brain Res* 69: 594–612, 1988.

Müller MM, Junghöfer M, Elbert T, and Rockstroh B. Visually induced gamma-band responses to coherent and incoherent motion: a replication study. *Neuroreport* 8: 2575–2579, 1997.

Murthy VN and Fetz EE. Coherent 25- to 35-Hz oscillations in the sensorimotor cortex of awake behaving monkeys. *Proc Natl Acad Sci USA* 89: 5670–5674, 1992.

Nase G, Monyer H, Brecht M, Singer W, and Engel AK. The mouse model permits the study of cellular mechanisms underlying neuronal synchrony in visual cortex. *Soc Neurosci Abstr* 25: 676, 1999.

Neuenschwander S and Singer W. Long-range synchronization of oscillatory light responses in the cat retina and lateral geniculate nucleus. *Nature* 379: 728–733, 1996.

Neuenschwander S and Varela FJ. Visually triggered neuronal oscillations in the pigeon: an autocorrelation study of tectal activity. *Eur J Neurosci* 5: 870–881, 1993.

Nicolelis MAL, Baccala LA, Lin RCS, and Chapin JK. Sensorimotor encoding by synchronous neural ensemble activity at multiple levels of the somatosensory system. *Science* 268: 1353–1358, 1995.

Pantev C, Makeig S, Hoke M, Galambos R, Hampson S, and Gallen C. Human auditory evoked gamma-band magnetic fields. *Proc Natl Acad Sci U S A* 88: 8996–9000, 1991.

Prechtl JC. Visual motion induces synchronous oscillations in turtle visual cortex. *Proc Natl Acad Sci USA* 91: 12467–12471, 1994.

Pulvermüller F, Lutzenberger W, Preissl H, and Birbaumer N. Spectral responses in the gamma-band: physiological signs of higher cognitive processes? *Neuroreport* 6: 2059–2064, 1995.

Riehle A, Grün S, Diesmann M, and Aertsen A. Spike synchronization and rate modulation differentially involved in motor cortical function. *Science* 278: 1950–1953, 1997.

Rodriguez E, George N, Lachaux JP, Martinerie J, Renault B, and Varela FJ. Perception's shadow: long-distance synchronization of human brain activity. *Nature* 397: 430–433, 1999.

Sanes JN and Donoghue JP. Oscillations in local field potentials of the primate motor cortex during voluntary movement. *Proc Natl Acad Sci USA* 90: 4470–4474, 1993.

Singer W. Neuronal synchrony: a versatile code for the definition of relations? *Neuron* 24: 49–65, 1999.

Singer W and Gray CM. Visual feature integration and the temporal correlation hypothesis. *Annu Rev Neurosci* 18: 555–586, 1995.

Steriade M, Amzica F, and Contreras D. Synchronization of fast (30–40 Hz) spontaneous cortical rhythms during brain activation. *J Neurosci* 16: 392–417, 1996.

Tallon-Baudry C and Bertrand O. Oscillatory gamma activity in humans and its role in object representation. *Trends Cogn Sci* 3: 151–162, 1999.

Tallon-Baudry C, Bertrand O, Delpuech C, and Pernier J. Oscillatory γ-band (30–70 Hz) activity induced by a visual search task in humans. *J Neurosci* 17: 722–734, 1997.

Vaadia E, Haalman I, Abeles M, Bergman H, Prut Y, Slovin H, and Aertsen A. Dynamics of neuronal interactions in monkey cortex in relation to behavioural events. *Nature* 373: 515–518, 1995.

Wagor E, Mangini NJ, and Pearlman AL. Retinotopic organization of striate and extrastriate visual cortex in the mouse. *J Comp Neurol* 193: 187–202, 1980.